2-24-2017

Binding of nitric oxide in CDGSH-type [2Fe-2S] clusters of the human mitochondrial protein miner2

Zishuo Cheng
Louisiana State University

Aaron P. Landry
Louisiana State University

Yiming Wang
Louisiana State University

Huangen Ding
Louisiana State University

Recommended Citation

Cheng, Z., Landry, A., Wang, Y., & Ding, H. (2017). Binding of nitric oxide in CDGSH-type [2Fe-2S] clusters of the human mitochondrial protein miner2. *Journal of Biological Chemistry, 292* (8), 3146-3153. https://doi.org/10.1074/jbc.M116.766774

THE JOURNAL OF BIOLOGICAL CHEMISTRY VOL. 292, NO. 8, pp. 3146–3153, February 24, 2017

Binding of Nitric Oxide in CDGSH-type [2Fe-2S] Clusters of the Human Mitochondrial Protein Miner2*[S]

Received for publication, November 7, 2016, and in revised form, January 10, 2017 Published, JBC Papers in Press, January 12, 2017, DOI 10.1074/jbc.M116.766774

Zishuo Cheng, Aaron P. Landry, Yiming Wang, and Huangen Ding[1]

From the Department of Biological Sciences, Louisiana State University, Baton Rouge, Louisiana 70803

Edited by John M. Denu

Iron-sulfur proteins are among the primary targets of nitric oxide in cells. Previous studies have shown that iron-sulfur clusters hosted by cysteine residues in proteins are readily disrupted by nitric oxide forming a protein-bound dinitrosyl iron complex, thiolate-bridged di-iron tetranitrosyl complex, or octanitrosyl cluster. Here we report that human mitochondrial protein Miner2 [2Fe-2S] clusters can bind nitric oxide without disruption of the clusters. Miner2 is a member of a new CDGSH iron-sulfur protein family that also includes two mitochondrial proteins: the type II diabetes-related mitoNEET and the Wolfram syndrome 2-linked Miner1. Miner2 contains two CDGSH motifs, and each CDGSH motif hosts a [2Fe-2S] cluster via three cysteine and one histidine residues. Binding of nitric oxide in the reduced Miner2 [2Fe-2S] clusters produces a major absorption peak at 422 nm without releasing iron or sulfide from the clusters. The EPR measurements and mass spectrometry analyses further reveal that nitric oxide binds to the reduced [2Fe-2S] clusters in Miner2, with each cluster binding one nitric oxide. Although the [2Fe-2S] cluster in purified human mitoNEET and Miner1 fails to bind nitric oxide, a single mutation of Asp-96 to Val in mitoNEET or Asp-123 to Val in Miner1 facilitates nitric oxide binding in the [2Fe-2S] cluster, indicating that a subtle change of protein structure may switch mitoNEET and Miner1 to bind nitric oxide. The results suggest that binding of nitric oxide in the CDGSH-type [2Fe-2S] clusters in mitochondrial protein Miner2 may represent a new nitric oxide signaling mode in cells.

Iron-sulfur clusters in proteins are often hosted by cysteine residues, although histidine, glutamine, serine, or arginine can also be the ligands (1, 2). Recently, a new group of iron-sulfur proteins that contain one or two CDGSH motifs have been identified in eukaryotes, archaea, and several bacteria (3). A common feature of the CDGSH proteins is that they host one or two [2Fe-2S] clusters via an unusual ligand arrangement of three cysteine and one histidine residues (3). In human mitochondria, there are three CDGSH iron-sulfur domain (CISD)[2] proteins: mitoNEET (CISD1) (4), Miner1 (mitoNEET-related protein 1, CISD2, or NAF-1) (5, 6), and Miner2 (mitoNEET-related protein 2, CISD3) (7). MitoNEET, a target of the type II diabetes drug pioglitazone (4), localizes on the mitochondrial outer membrane and exists as a homodimer (7). Each monomer of mitoNEET contains a CDGSH motif that hosts one [2Fe-2S] cluster (8–10). Miner1 has 54% identity and 76% similarity with mitoNEET (5) and also localizes on the mitochondrial outer membrane (11). Like mitoNEET, each monomer of the Miner1 homodimer contains a CDGSH motif that hosts one [2Fe-2S] cluster (5). Mutation of Miner1 has been attributed to causing Wolfram syndrome 2, a disease characterized by juvenile-onset diabetes mellitus and optic atrophy (12). Both mitoNEET and Miner1 have central roles in regulating iron homeostasis, energy metabolism, and production of free radicals in mitochondria (11, 13). Recent studies further suggested that mitoNEET may transfer its [2Fe-2S] clusters to target proteins in the cytoplasm (14, 15) or directly regulate mitochondrial functions via the redox transition of the [2Fe-2S] clusters (16–18). Miner2 contains an N-terminal mitochondrial signal peptide and two CDGSH motifs. Although mitochondrial Miner2 is found to be highly expressed in lung cancer, breast cancer, and other types of cancer (Cancer Browser), it has not been purified or characterized previously, and very little is known about the function of Miner2 in mitochondria. Nevertheless, the crystal structure of the Miner2 homolog from *Magnetospirillum magneticum* shows that Miner2 is a monomer that hosts two [2Fe-2S] clusters via two CDGSH motifs in an internal pseudodyad symmetry (3).

Ironically, iron-sulfur clusters are among the primary targets of the physiological free radical nitric oxide, as nitric oxide has a strong reactivity with ferrous iron in proteins (19). In bacteria, nitric oxide regulates global gene expression via direct modification of iron-sulfur clusters in several transcription factors (20–24). At high concentrations, nitric oxide inhibits bacterial cell growth by disrupting iron-sulfur clusters in multiple enzymes (21, 25, 26). In mitochondria, nitric oxide has been shown to modulate energy metabolism by interacting with iron-sulfur clusters and hemes in proteins (27). For example, nitric oxide directly modifies the [4Fe-4S] cluster in mitochondrial aconitase and blocks the citric acid cycle (28). Among the reported examples so far, iron-sulfur clusters in proteins are all

* This research was supported in part by National Institutes of Health Grant R15GM109399 and American Heart Association Grant 13GRNT16890014. The authors declare that they have no conflicts of interest with the contents of this article. The content is solely the responsibility of the authors and does not necessarily represent the official views of the National Institutes of Health.

[S] This article contains supplemental Figs. 1 and 2.

[1] To whom correspondence should be addressed: Dept. of Biological Sciences, Louisiana State University, Baton Rouge, LA 70803. E-mail: hding@lsu.edu.

[2] The abbreviations used are: CISD, CDGSH iron-sulfur domain; diethylamine NONOate, diethylammonium (Z)-1-(*N*,*N*-diethylamino)diazen-1-ium-1,2-diolate.

disrupted by nitric oxide forming a protein-bound dinitrosyl iron complex (25–29), thiolate-bridged di-iron tetranitrosyl complex (30, 31), or octanitrosyl cluster (32), depending on specific proteins and experimental conditions. In all of these examples, iron-sulfur clusters in proteins are hosted by either cysteine residues (33) or Rieske-type two histidine and two cysteine residues (34). Here, we report that the CDGSH-type [2Fe-2S] clusters in the human mitochondrial protein Miner2 can bind nitric oxide without disruption of the clusters. Although the [2Fe-2S] cluster in purified human mitoNEET and Miner1 fails to bind nitric oxide, a single mutation of Asp-96 to Val in mitoNEET or Asp-123 to Val in Miner1 facilitates nitric oxide binding in the [2Fe-2S] clusters, indicating that a subtle change of protein structure may switch mitoNEET and Miner1 to bind nitric oxide at the [2Fe-2S] cluster. The results suggest that binding of nitric oxide in the CDGSH-type [2Fe-2S] clusters in mitochondrial protein Miner2 may represent a novel nitric oxide signaling mode in cells.

Results

Human Miner2 [2Fe-2S] Clusters Have a Unique Interaction with Nitric Oxide—The recombinant human mitochondrial CDGSH proteins mitoNEET, Miner1, and Miner2 were prepared from *Escherichia coli* cells as described under "Experimental Procedures." Fig. 1*A* shows that purified human mitoNEET, Miner1, and Miner2 had a similar UV-visible absorption spectrum, with two major absorption peaks at 458 and 550 nm, indicative of the oxidized [2Fe-2S] clusters in each protein (35). When purified proteins were reduced with dithiothreitol under anaerobic conditions (17), mitoNEET and Miner1 had an identical EPR spectrum with g = 1.94 of the reduced [2Fe-2S] clusters (Fig. 1*B*), as reported previously (35, 36). This is likely because mitoNEET and Miner1 have 54% identity and 76% similarity (5). In contrast, the reduced Miner2 appeared to have two overlapping EPR spectra (Fig. 1*B*). Deconvolution of the EPR spectrum of the reduced Miner2 produced two distinct EPR spectra with g = 1.92 and g = 1.94, respectively (Fig. 1*C*), suggesting that human Miner2, like the Miner2 homolog from *M. magneticum* (3), hosts two [2Fe-2S] clusters via two CDGSH motifs.

As the redox midpoint potential (E_{m7}) of the [2Fe-2S] cluster in mitoNEET is about 0 mV (37), the CDGSH-type [2Fe-2S] clusters in proteins are most likely in a reduced state in cells under normal physiological conditions (17). To explore the interaction between the mitochondrial CDGSH proteins and nitric oxide, purified mitoNEET, Miner1, and Miner2 were pre-reduced with dithiothreitol before being exposed to nitric oxide under anaerobic conditions. When reduced mitoNEET or Miner1 was treated with a 2-fold excess of nitric oxide (from a nitric oxide gas-saturated solution), the UV-visible absorption spectrum of the [2Fe-2S] cluster in mitoNEET (Fig. 2*A*) or Miner1 (Fig. 2*B*) was not significantly changed, indicating that the [2Fe-2S] cluster in mitoNEET or Miner1 did not interact with nitric oxide under the experimental conditions. In contrast, when reduced Miner2 was treated with a 2-fold excess of nitric oxide, a new absorption peak at 422 nm appeared (Fig. 2*C*). No detectable amount of iron or sulfide was released from the Miner2 [2Fe-2S] clusters after nitric oxide treatment (data not shown), indicating that nitric oxide may bind to the Miner2 [2Fe-2S] clusters without disrupting them. In a control experiment, when reduced apo-Miner2 (Miner2 without the [2Fe-2S] clusters) was treated with a 2-fold excess of nitric oxide under anaerobic conditions, no absorption peak at 422 nm was observed (data not shown), further suggesting that the absorption peak at 422 nm is likely due to the interaction between the Miner2 [2Fe-2S] clusters and nitric oxide.

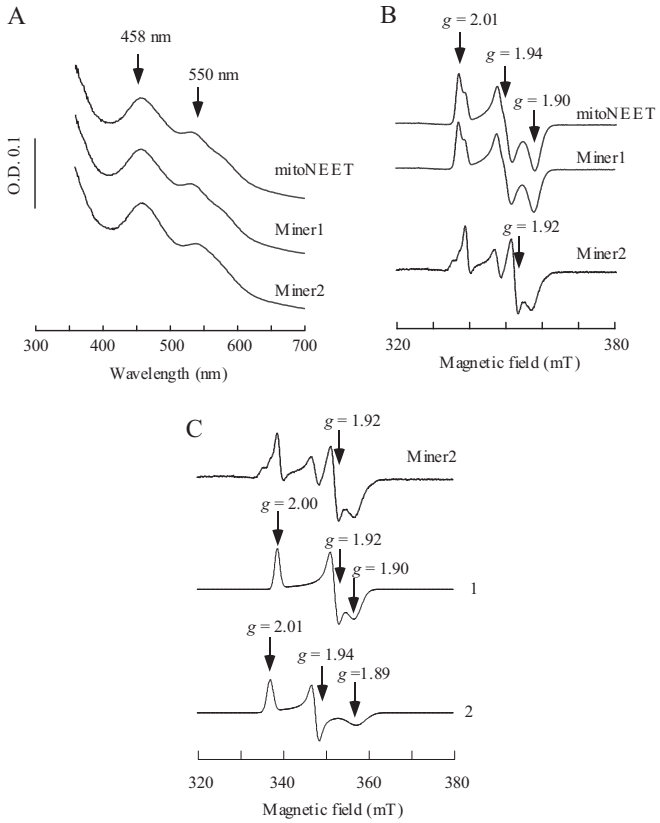

FIGURE 1. **UV-visible and EPR spectra of human mitoNEET, Miner1, and Miner2.** *A*, UV-visible absorption spectra of purified mitoNEET, Miner1, and Miner2. MitoNEET, Miner1, and Miner2 were purified as described under "Experimental Procedures." Each protein (containing 20 μM [2Fe-2S] cluster) was dissolved in buffer containing NaCl (500 mM) and Tris (20 mM (pH 8.0)). *O.D.*, optical density. *B*, EPR spectra of purified human mitoNEET, Miner1, and Miner2. Each protein (containing 20 μM [2Fe-2S] cluster) was dissolved in buffer containing NaCl (500 mM) and Tris (20 mM (pH 8.0)) and reduced with dithiothreitol (4 mM) under anaerobic conditions. *mT*, millitesla. *C*, EPR spectra of Miner2. *Top spectrum*, dithiothreitol-reduced Miner2 [2Fe-2S] clusters. *Spectra 1* and *2* were the results of the deconvolution of the *top spectrum* using simulation software. The g values of the deconvoluted spectra are shown.

Under the same experimental conditions, *E. coli* SoxR, which hosts a [2Fe-2S] cluster via four cysteine residues (38), was treated with a 2-fold excess of nitric oxide under anaerobic conditions. Fig. 2*D* shows that the absorption peaks at 414 and 462 nm of the SoxR [2Fe-2S] clusters were largely eliminated, with no appearance of the absorption peak at 422 nm after nitric oxide treatment, confirming that the SoxR [2Fe-2S] clusters were disrupted by nitric oxide forming a protein-bound dinitrosyl iron complex, as reported previously (20). Thus, the Miner2 [2Fe-2S] clusters have a unique interaction with nitric oxide.

The Miner2 [2Fe-2S] Clusters Have a Strong Binding Affinity for Nitric Oxide—To further explore the interaction between the Miner2 [2Fe-2S] clusters and nitric oxide, Miner2 was pre-

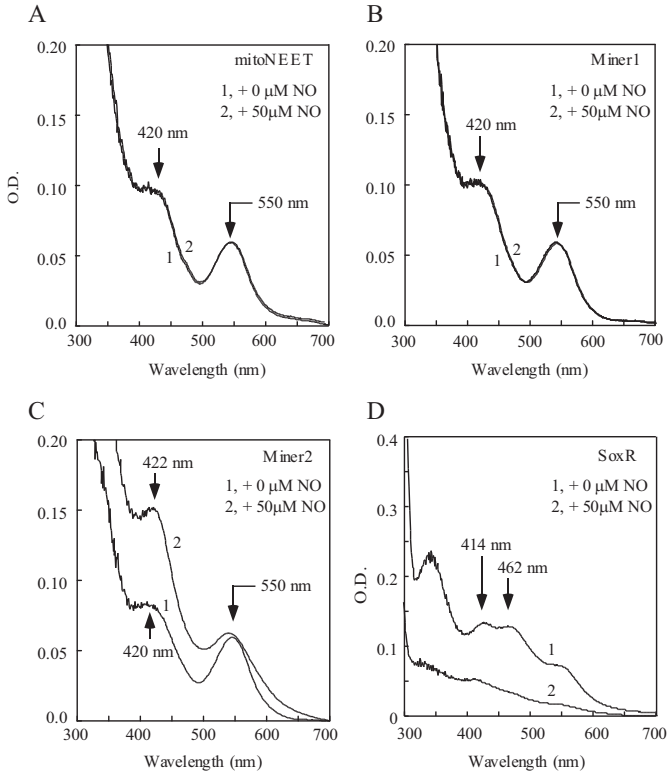

FIGURE 2. **Nitric oxide binding in human mitoNEET, Miner1 and Miner2.** *A*, purified mitoNEET (containing 20 μM [2Fe-2S] cluster) in buffer containing NaCl (500 mM) and Tris (20 mM (pH 8.0)) was reduced with dithiothreitol (4 mM) under anaerobic conditions before (*spectrum 1*) and after (*spectrum 2*) addition of 40 μM nitric oxide anaerobically. *O.D.*, optical density. *B*, the same as in *A*, except purified Miner1 was used. *C*, the same as in *A*, except purified Miner2 was used. *D*, the same as in *A*, except purified *E. coli* SoxR was used.

reduced with dithiothreitol, followed by stepwise addition of nitric oxide under anaerobic conditions. UV-visible absorption spectra were taken after each addition of nitric oxide. Fig. 3*A* shows that, as the nitric oxide concentration increased in the incubation solution, the absorption peak at 422 nm gradually increased. The amplitude of the absorption peak at 422 nm was almost linearly proportional to the nitric oxide concentration in the incubation solution. An about 2-fold excess of nitric oxide over Miner2 was sufficient to saturate the nitric oxide binding in the Miner2 [2Fe-2S] clusters (Fig. 3*B*), indicating that the Miner2 [2Fe-2S] clusters have a strong binding affinity for nitric oxide.

In parallel experiments, after reduced Miner2 was treated with stepwise addition of nitric oxide under anaerobic conditions, samples were immediately frozen in liquid nitrogen and subjected to EPR measurements. Fig. 3*C* shows that, as nitric oxide concentration increased in the incubation solution, the EPR signal at g = 1.92 of the reduced Miner2 [2Fe-2S] clusters gradually decreased. At 2-fold excess of nitric oxide over Miner2, the EPR signal at g = 1.92 was largely eliminated. A small EPR signal at g = 2.03, indicative of a protein-bound dinitrosyl iron complex (26, 28), appeared after the Miner2 was treated with nitric oxide (Fig. 3*C*). However, spin quantification of the EPR signal at g = 2.04 showed that less than 5% of the reduced Miner2 [2Fe-2S] clusters might be converted to the dinitrosyl iron complex, suggesting that the majority of the reduced Miner2 [2Fe-2S] clusters became EPR-silent after being treated with a 2-fold excess of nitric oxide.

To further test the idea that nitric oxide binds to the Miner2 [2Fe-2S] clusters, the nitric oxide-treated Miner2 was repurified from the incubation solution by passing the protein sample through a High-Trap desalting column. Repurified Miner2 was then treated with 0.2 M HCl to release the acid-labile iron and sulfide from iron-sulfur clusters in the protein. Fig. 3*D* shows that more than 80% of the acid-labile iron and sulfide content remained with Miner2 after being treated with a 2-fold excess of nitric oxide. Thus, nitric oxide may eliminate the EPR signal at g = 1.92 of the reduced Miner2 [2Fe-2S] clusters by directly binding to the clusters.

Mass Spectrometry Analyses of the Nitric Oxide-bound Miner2—L-cysteine has been used to release nitric oxide (in the form of nitrite) from the protein-bound dinitrosyl iron complex under aerobic conditions (26). To probe the nitric oxide binding in the Miner2 [2Fe-2S] clusters, the nitric oxide-treated Miner2 was repurified and incubated with L-cysteine at 37 °C under aerobic conditions for 30 min. Nitrite released from Miner2 was measured using Griess reagents (26). Fig. 3*D* shows that nitrite was indeed released when the nitric oxide-treated Miner2 was incubated with 10 mM L-cysteine under aerobic conditions. The ratio of nitrite to total iron in the nitric oxide-treated Miner2 was about 0.41 ± 0.12, indicating that each [2Fe-2S] cluster in Miner2 binds about one nitric oxide. For Miner2 without nitric oxide treatment, no detectable amount of nitrite was observed after incubation with 10 mM L-cysteine.

Mass spectrometry was further used to analyze the nitric oxide binding in the Miner2 [2Fe-2S] clusters. Fig. 4*A* shows that purified Miner2 had a major peak at a molecular weight of 10,878, which is the sum of the expected molecular weight of apo-Miner2 (10,526) plus 2 × [2Fe-2S] clusters (352). When Miner2 was exposed to a 2-fold excess of nitric oxide, the peak at 10,878 was largely eliminated and replaced with two new peaks at molecular weights of 10,878 + 30 and 10,878 + 60, respectively (Fig. 4*A*). As the molecular weight of nitric oxide is 30, two new peaks were assigned to the Miner2 with only one [2Fe-2S] cluster bound with nitric oxide and the one with both [2Fe-2S] clusters bound with nitric oxide, respectively. Missing a nitric oxide in the Miner2 [2Fe-2S] clusters could be because, during ionization in the mass spectrometry analysis, some nitric oxide was released from the clusters.

A minor peak at a molecular weight of 10,526 representing apo-Miner2 was also observed in the same mass spectrum (Fig. 4*B*). Unlike the major peak at 10,878 (the Miner2 [2Fe-2S] clusters), the minor peak at 10,536 (apo-Miner2) was not changed after nitric oxide treatment (Fig. 4*B*), suggesting that apo-Miner2 did not bind or react with nitric oxide under the experimental conditions.

A Single Amino Acid Mutation in mitoNEET and Miner1 Facilitates Nitric Oxide Binding in the [2Fe-2S] Cluster—Like Miner2, mitoNEET and Miner1 contain a CDGSH motif that hosts a [2Fe-2S] cluster via three cysteine and one histidine residues (5, 8–10). However, unlike the reduced Miner2 [2Fe-2S] clusters, the reduced mitoNEET [2Fe-2S] cluster or Miner1 [2Fe-2S] cluster fails to bind nitric oxide (Fig. 2, *A* and *B*). One possible explanation is that, in purified mitoNEET and Miner1,

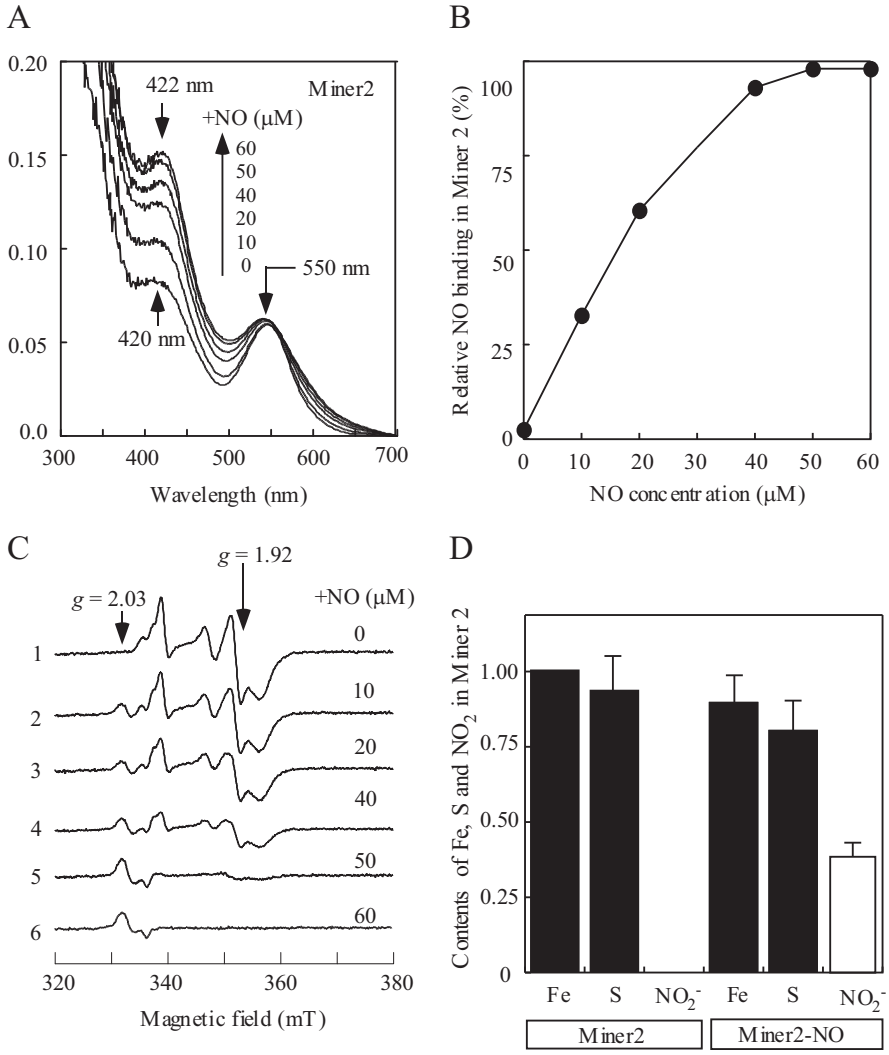

FIGURE 3. **The nitric oxide binding activity of Miner2.** *A*, UV-visible absorption spectra of Miner2. Purified Miner2 (containing 20 μM [2Fe-2S] cluster) was prereduced with dithiothreitol (4 mM) under anaerobic conditions, followed by stepwise addition of nitric oxide (from a nitric oxide-saturated solution) anaerobically. Spectra were taken after each addition of nitric oxide. *B*, the amplitudes of the absorption peak at 422 nm of the Miner2 [2Fe-2S] clusters were plotted as a function of the nitric oxide concentrations in incubation solutions. The results are representative of three independent experiments. *C*, EPR spectra of Miner2. Purified Miner2 (containing 20 μM [2Fe-2S] cluster) was prereduced with dithiothreitol (4 mM) under anaerobic conditions, followed by stepwise addition of nitric oxide anaerobically. Samples were immediately frozen in liquid nitrogen and subjected to the EPR measurements. *mT*, millitesla. *D*, iron, sulfide, and nitrite content analyses of Miner2. Miner2 was repurified after treatment of a 2-fold excess of nitric oxide under anaerobic conditions. The amounts of iron, sulfide, and nitrite were measured as described under "Experimental Procedures." In three different preparations, the iron content in Miner2 varied from 3.5 to 2.0 iron atoms per Miner2. For each preparation of Miner2, the ratio of iron to Miner2 was set to 1.0, and other content was calculated based on the ratio of iron to Miner2. The amount of nitrite in the Miner2 sample without nitric oxide treatment was not detectable. Data are mean ± S.D. from three experiments.

the protein conformation does not favor nitric oxide binding to the [2Fe-2S] clusters in the protein. Based on the crystal structure of mitoNEET (8–10), the [2Fe-2S] cluster is buried inside the protein structure, and Asp-96 is in the vicinity of the [2Fe-2S] cluster and potentially blocks the access of nitric oxide to the [2Fe-2S] cluster in mitoNEET (supplemental Figs. 2*A* and 2*B*). To test this idea, a mitoNEET mutant in which Asp-96 was replaced with Val (D96V) was constructed using site-directed mutagenesis. Fig. 5*B* shows that the reduced [2Fe-2S] cluster in the mitoNEET mutant (D96V) could indeed bind nitric oxide under anaerobic conditions. The mass spectrometry analysis further revealed that the mitoNEET mutant binds one nitric oxide per [2Fe-2S] cluster (supplemental Fig. 2*C*). Similar results were also observed in the Miner1 mutant in which Asp-123 (corresponding to Asp-96 of mitoNEET) was mutated to Val (data not shown). Thus, with a subtle structural change, the [2Fe-2S] cluster in mitoNEET and Miner1 has a similar nitric oxide binding activity as the Miner2 [2Fe-2S] clusters.

Discussion

Hemes and iron-sulfur clusters are the major iron-containing co-factors in proteins and are also the primary targets of nitric oxide (19). Although nitric oxide binding in ferrous heme iron in proteins has been extensively investigated and well understood (19, 27), much less has been known about the interactions between nitric oxide and iron-sulfur clusters in proteins. In previous studies, iron-sulfur clusters in proteins were found to be completely disrupted by nitric oxide forming a protein-bound dinitrosyl iron complex (25–29), thiolate-bridged di-iron tetranitrosyl complex (30, 31), or octanitrosyl cluster

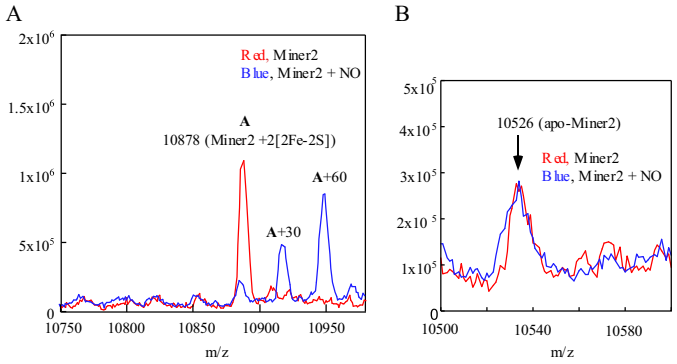

FIGURE 4. **Mass spectra of human Miner2 before and after nitric oxide treatment.** Purified Miner2 (containing 20 μM [2Fe-2S] cluster) was reduced with dithiothreitol (4 mM) under anaerobic conditions, followed by treatment with 50 μM nitric oxide. Miner2 was then repurified from the incubation solution and subjected to mass spectrometry analyses. *A*, deconvoluted mass spectra of the Miner2 [2Fe-2S] clusters before and after nitric oxide treatment. *B*, deconvoluted mass spectra of apo-Miner2 before and after nitric oxide treatment. *Red curve*, Miner2 before nitric oxide treatment; *blue curve*, Miner2 after nitric oxide treatment.

(32), depending on specific proteins and experimental conditions. Such modifications of iron-sulfur clusters by nitric oxide have also been demonstrated in iron-sulfur cluster model compounds (39, 40). However, in all of these reported examples, iron-sulfur clusters in proteins are hosted by either all cysteine residues (33) or Rieske-type two histidine and two cysteine residues (34). Our finding that the reduced CDGSH-type [2Fe-2S] clusters of human mitochondrial protein Miner2 are able to bind nitric oxide without disruption of the clusters represents a new interaction between nitric oxide and iron-sulfur clusters in proteins. In the CDGSH-type [2Fe-2S] cluster, which is hosted by three cysteine and one histidine residues, two iron atoms are asymmetric as one iron is bound by two cysteine residues and the other by one cysteine and one histidine residues (Fig. 6). When the [2Fe-2S] cluster is oxidized, both iron atoms in the cluster are in a ferric state. When the [2Fe-2S] cluster is reduced, the histidine-bound iron atom will be in a ferrous state (41). Because nitric oxide prefers to bind ferrous iron (19), we propose that the ferrous iron in the reduced Miner2 [2Fe-2S] clusters is likely the nitric oxide binding site (Fig. 6). The observed absorption peak at 422 nm of the reduced Miner2 [2Fe-2S] clusters after nitric oxide treatment (Fig. 2*C*) may represent the Soret absorption for the interaction between nitric oxide and the ferrous iron of the [2Fe-2S] clusters in Miner2. A similar Soret absorption around 420 nm has been attributed to nitric oxide binding to the ferrous heme iron in the heme nitric oxide/oxygen binding protein isolated from *Clostridium botulinum* (42) and in the thiolate-ligated ferrous cytochrome P450 of the neuronal nitric oxide synthase (43). Binding of nitric oxide in the Miner2 [2Fe-2S] clusters apparently changes the redox state of the ferrous iron of the clusters, as binding of nitric oxide eliminates the EPR signal at g = 1.92 of the reduced Miner2 [2Fe-2S] clusters (Fig. 3*C*). We also noticed that the interaction between nitric oxide and the Miner2 [2Fe-2S] clusters is stable, as the nitric oxide-bound Miner2 [2Fe-2S] clusters can be purified and directly observed from the mass spectrometry analysis (Fig. 4*A*). Although additional spectroscopic studies are needed to further illustrate the nitric oxide binding in the Miner2 [2Fe-2S] clusters, we postulate that binding of nitric oxide in the Miner2 [2Fe-2S] clusters may regulate the function of the protein in mitochondria.

Unlike the reduced [2Fe-2S] clusters in Miner2, the reduced [2Fe-2S] cluster in mitoNEET or Miner1 fails to bind nitric oxide (Fig. 2). Nevertheless, a single mutation of Asp-96 to Val in mitoNEET facilitates nitric oxide binding in the [2Fe-2S] cluster (Fig. 5). Similarly, the [2Fe-2S] cluster in the Miner1 mutant with Asp-123 mutated to Val (corresponding to Asp-96 of mitoNEET) can also bind nitric oxide. These results suggest that a subtle change in protein structure may switch mitoNEET and Miner1 to facilitate nitric oxide binding in the [2Fe-2S] clusters. As mitoNEET and Miner1 have specific interactions with multiple mitochondrial proteins, including the Parkinson's disease-associated protein Parkin (44, 45), such protein-protein interactions may well change the conformation of mitoNEET and Miner1 and facilitate the [2Fe-2S] cluster to bind nitric oxide. It is also possible that posttranslational modifications such as phosphorylation and acetylation of mitoNEET and Miner1 may promote nitric oxide binding in the [2Fe-2S] cluster. Although both mitoNEET and Miner1 are considered to be the central regulators for energy metabolism, iron homeostasis, and production of reactive oxygen species in mitochondria (13), the specific function of the [2Fe-2S] clusters in mitoNEET and Miner1 remains largely elusive. Recent studies have suggested that mitoNEET may transfer its [2Fe-2S] clusters to target proteins in the cytoplasm to promote iron-sulfur cluster biogenesis in the cytoplasm (14, 15). Alternatively, mitoNEET may directly regulate mitochondrial functions via redox transition of its [2Fe-2S] clusters (16–18). In either case, binding of nitric oxide in the [2Fe-2S] cluster in mitoNEET or Miner1 could potentially modulate the functions of these mitochondrial proteins. There are at least 60 more proteins that may host one or more [2Fe-2S] clusters via three cysteine and one histidine residues in human cells (46). Whether the [2Fe-2S] clusters in these newly identified proteins can bind nitric oxide remains to be investigated.

To conclude, human mitochondrial protein Miner2 [2Fe-2S] clusters can bind nitric oxide without disruption of the clusters. Although the [2Fe-2S] cluster in purified mitoNEET and Miner1 fails to bind nitric oxide, a subtle structural change in these proteins can facilitate nitric oxide binding in the [2Fe-2S] cluster. Binding of nitric oxide in the CDGSH-type [2Fe-2S] clusters of mitochondrial proteins may represent a new nitric oxide signaling mode to modulate mitochondrial functions in human cells.

Experimental Procedures

Protein Preparation—The DNA fragments encoding human mitochondrial CDGSH-type iron-sulfur proteins (mitoNEET, containing residues 33–108 (4); Miner1, containing residues 57–135 (5); and Miner2 (containing residues 36–127)), were synthesized (Genscript Co.) and cloned into the pET28b+ plasmid for expression in *E. coli* cells. The MitoNEET mutant and Miner1 mutant were constructed using a site-directed mutagenesis kit (Agilent Co.). The cloned DNA sequences were confirmed by direct sequencing (Eurofins MWG Operon). *E. coli* cells containing expression plasmids were diluted 1:100 overnight in freshly prepared Luria-Bertani medium and incu-

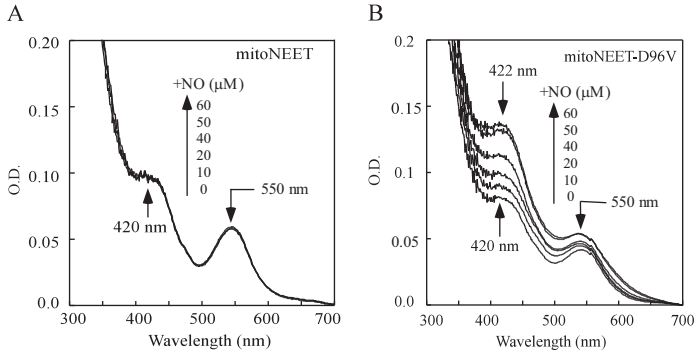

FIGURE 5. **Nitric oxide binding in the [2Fe-2S] cluster of the mitoNEET mutant D96V.** Purified mitoNEET (containing 20 μM [2Fe-2S] cluster) in buffer containing NaCl (500 mM) and Tris (20 mM (pH 8.0)) was reduced with dithiothreitol (4 mM) under anaerobic conditions, followed by stepwise addition of nitric oxide (from a nitric oxide-saturated solution). Spectra were taken after each addition of nitric oxide. Final concentrations of nitric oxide are shown. *O.D.*, optical density. *B*, the same as *A*, except mitoNEET was replaced with the mitoNEET-D96V in the incubation solutions.

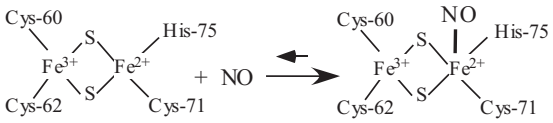

FIGURE 6. **Proposed model for nitric oxide binding in the reduced Miner2 [2Fe-2S] clusters.** There are two [2Fe-2S] clusters in each Miner2. The first [2Fe-2S] cluster hosted by three cysteine and one histidine residues in Miner2 is shown. For the reduced Miner2 [2Fe-2S] cluster, the iron atom bound with His/Cys residues is in a ferrous state, and nitric oxide binds the ferrous iron in the [2Fe-2S] cluster.

bated at 37 °C with aeration (250 rpm) for 3 h, followed by protein induction using isopropyl 1-thio-β-D-galactopyranoside (100 μM) overnight at 18 °C. Apo-Miner2 (Miner2 without iron-sulfur clusters) was prepared following the same procedures, except 0.5 mM dipyridyl was added to the Luria-Bertani medium 15 min before isopropyl 1-thio-β-D-galactopyranoside was added to induce the expression of Miner2 in *E. coli* cells. Protein was purified as described previously (35). The purity of purified proteins was greater than 95%, as judged by electrophoresis analysis on a 15% polyacrylamide gel containing SDS followed by staining with Coomassie Blue. The UV-visible absorption spectra were recorded in a Beckman DU640 UV-visible absorption spectrometer equipped with a temperature controller. The full UV-visible absorption spectrum and SDS-PAGE of purified human Miner2 are shown in supplemental Fig. 1.

Nitric Oxide Solution Preparation—Nitric oxide gas (Air Co.) was first passed through a soda-lima column to remove NO_2 and higher nitrogen oxides before being used to bubble predegassed water in a sealed 50-ml flask for 5 min. The concentration of nitric oxide in the nitric oxide-saturated solution was measured using a nitric oxide electrode (World Precision Instruments) (33). The nitric oxide-releasing reagent diethylamine NONOate (Cayman Chemicals) was also used for preparing nitric oxide solutions. Diethylamine NONOate was first dissolved in buffer containing Tris (20 mM (pH 10.5)). The NONOate concentration was determined from the absorption peak at 250 nm using an extinction coefficient of 6.5 $mM^{-1}cm^{-1}$. Diethylamine NONOate releases 1.5 mol of nitric oxide at a half-life time of 2 min at 37 °C (pH 7.4). Similar results were obtained when the nitric oxide gas solution or the NONOate solution was used in the experiments.

Iron, Sulfide, and Nitrite Determinations—The total acid-labile iron content in protein samples was determined using an iron indicator, FerroZine, following the procedures described in Ref. 47. The total acid-labile sulfide content in protein samples was determined following the procedures described by Siegel (48). Nitric oxide bound in Miner2 was released by incubating the protein with 10 mM L-cysteine at 37 °C for 30 min under aerobic conditions. The total nitrite content in samples was measured using Griess reagents according to the instructions of the manufacturer (Cayman Chemicals) (26). The detection limit of the Griess assay for nitrite was about 1.0 μM. The ratios of iron, sulfide, and nitrite to monomeric Miner2 are presented.

EPR Measurements—The X-band EPR spectra were recorded using a Bruker model ESR-300 spectrometer equipped with an Oxford Instruments 910 continuous flow cryostat. Routine EPR conditions were as follows: microwave frequency, 9.47 GHz; microwave power, 10.0 milliwatt; modulation frequency, 100 kHz; modulation amplitude, 1.2 millitesla; temperature, 20 K; receiver gain, 2×10^5. The EPR spectrum simulation software was kindly provided by Dr. Evert Duin (Auburn University).

Mass Spectrometry Measurements—All experiments were performed with an AmaZon speed electron transfer dissociation (ETD) ion trap mass spectrometer (Bruker Daltonics, Billerica, MA). Sample solution was infused via an Apollo II electrospray ion source using a syringe pump at a flow rate of 5 μl/min. MS detection was performed in a full-scan mode in positive ionization-enhanced resolution mode with a scan speed of 8100 m/z/s. The parameter settings for electrospray ionization-mass spectrometry (ESI-MS) were as follows: capillary voltage, 4500 V; end plate offset, −500 V; nebulizer, 8 p.s.i.; dry gas, 4 liters/min; dry gas temperature, 180 °C. MS data were acquired from 300 to 3000 with a target mass of 1500 m/z and trap drive level of 100%. The software used for data processing and deconvolution was Compass DataAnalysis (Bruker Daltonics).

Author Contributions—Z. C., A. P. L., Y. W., and H. D. designed, performed, and analyzed the experiments. All authors reviewed the results and approved the final version of the manuscript.

Acknowledgments—We thank Dr. Evert Duin (Auburn University) for sharing the simulation software for deconvoluting the EPR spectra of the reduced Miner2 [2Fe-2S] clusters. We also thank Dr. Jeonghoon Lee (Mass Spectrometry Facility, Louisiana State University) for assisting with the mass spectrometry analysis.

References

1. Meyer, J. (2008) Iron-sulfur protein folds, iron-sulfur chemistry, and evolution. *J. Biol. Inorg. Chem.* **13,** 157–170
2. Johnson, D. C., Dean, D. R., Smith, A. D., and Johnson, M. K. (2005) Structure, function, and formation of biological iron-sulfur clusters. *Annu. Rev. Biochem.* **74,** 247–281
3. Lin, J., Zhang, L., Lai, S., and Ye, K. (2011) Structure and molecular evolution of CDGSH iron-sulfur domains. *PLoS ONE* **6,** e24790
4. Colca, J. R., McDonald, W. G., Waldon, D. J., Leone, J. W., Lull, J. M., Bannow, C. A., Lund, E. T., and Mathews, W. R. (2004) Identification of a novel mitochondrial protein ("mitoNEET") cross-linked specifically by a thiazolidinedione photoprobe. *Am. J. Physiol. Endocrinol. Metab.* **286,** E252-E260
5. Conlan, A. R., Axelrod, H. L., Cohen, A. E., Abresch, E. C., Zuris, J., Yee, D., Nechushtai, R., Jennings, P. A., and Paddock, M. L. (2009) Crystal structure of Miner1: the redox-active 2Fe-2S protein causative in Wolfram syndrome 2. *J. Mol. Biol.* **392,** 143–153
6. Bai, F., Morcos, F., Sohn, Y. S., Darash-Yahana, M., Rezende, C. O., Lipper, C. H., Paddock, M. L., Song, L., Luo, Y., Holt, S. H., Tamir, S., Theodorakis, E. A., Jennings, P. A., Onuchic, J. N., Mittler, R., and Nechushtai, R. (2015) The Fe-S cluster-containing NEET proteins mitoNEET and NAF-1 as chemotherapeutic targets in breast cancer. *Proc. Natl. Acad. Sci. U.S.A.* **112,** 3698–3703
7. Wiley, S. E., Murphy, A. N., Ross, S. A., van der Geer, P., and Dixon, J. E. (2007) MitoNEET is an iron-containing outer mitochondrial membrane protein that regulates oxidative capacity. *Proc. Natl. Acad. Sci. U.S.A.* **104,** 5318–5323
8. Hou, X., Liu, R., Ross, S., Smart, E. J., Zhu, H., and Gong, W. (2007) Crystallographic studies of human MitoNEET. *J. Biol. Chem.* **282,** 33242–33246
9. Lin, J., Zhou, T., Ye, K., and Wang, J. (2007) Crystal structure of human mitoNEET reveals distinct groups of iron-sulfur proteins. *Proc. Natl. Acad. Sci. U.S.A.* **104,** 14640–14645
10. Paddock, M. L., Wiley, S. E., Axelrod, H. L., Cohen, A. E., Roy, M., Abresch, E. C., Capraro, D., Murphy, A. N., Nechushtai, R., Dixon, J. E., and Jennings, P. A. (2007) MitoNEET is a uniquely folded 2Fe 2S outer mitochondrial membrane protein stabilized by pioglitazone. *Proc. Natl. Acad. Sci. U.S.A.* **104,** 14342–14347
11. Sohn, Y. S., Tamir, S., Song, L., Michaeli, D., Matouk, I., Conlan, A. R., Harir, Y., Holt, S. H., Shulaev, V., Paddock, M. L., Hochberg, A., Cabanchick, I. Z., Onuchic, J. N., Jennings, P. A., Nechushtai, R., and Mittler, R. (2013) NAF-1 and mitoNEET are central to human breast cancer proliferation by maintaining mitochondrial homeostasis and promoting tumor growth. *Proc. Natl. Acad. Sci. U.S.A.* **110,** 14676–14681
12. Amr, S., Heisey, C., Zhang, M., Xia, X. J., Shows, K. H., Ajlouni, K., Pandya, A., Satin, L. S., El-Shanti, H., and Shiang, R. (2007) A homozygous mutation in a novel zinc-finger protein, ERIS, is responsible for Wolfram syndrome 2. *Am. J. Hum. Genet.* **81,** 673–683
13. Tamir, S., Paddock, M. L., Darash-Yahana-Baram, M., Holt, S. H., Sohn, Y. S., Agranat, L., Michaeli, D., Stofleth, J. T., Lipper, C. H., Morcos, F., Cabantchik, I. Z., Onuchic, J. N., Jennings, P. A., Mittler, R., and Nechushtai, R. (2015) Structure-function analysis of NEET proteins uncovers their role as key regulators of iron and ROS homeostasis in health and disease. *Biochim. Biophys. Acta* **1853,** 1294–1315
14. Golinelli-Cohen, M. P., Lescop, E., Mons, C., Gonçalves, S., Clémancey, M., Santolini, J., Guittet, E., Blondin, G., Latour, J. M., and Bouton, C. (2016) Redox control of the human iron-sulfur repair protein MitoNEET activity via its iron-sulfur cluster. *J. Biol. Chem.* **291,** 7583–7593
15. Zuris, J. A., Harir, Y., Conlan, A. R., Shvartsman, M., Michaeli, D., Tamir, S., Paddock, M. L., Onuchic, J. N., Mittler, R., Cabantchik, Z. I., Jennings, P. A., and Nechushtai, R. (2011) Facile transfer of [2Fe-2S] clusters from the diabetes drug target mitoNEET to an apo-acceptor protein. *Proc. Natl. Acad. Sci. U.S.A.* **108,** 13047–13052
16. Bak, D. W., and Elliott, S. J. (2013) Conserved hydrogen bonding networks of MitoNEET tune Fe-S cluster binding and structural stability. *Biochemistry* **52,** 4687–4696
17. Landry, A. P., and Ding, H. (2014) Redox control of human mitochondrial outer membrane protein MitoNEET [2Fe-2S] clusters by biological thiols and hydrogen peroxide. *J. Biol. Chem.* **289,** 4307–4315
18. Landry, A. P., Wang, Y., Cheng, Z., Crochet, R. B., Lee, Y. H., and Ding, H. (2017) Flavin nucleotides act as electron shuttles mediating reduction of the [2Fe-2S] clusters in mitochondrial outer membrane protein mitoNEET. *Free Radic Biol. Med.* **102,** 240–247
19. Cooper, C. E. (1999) Nitric oxide and iron proteins. *Biochim. Biophys. Acta* **1411,** 290–309
20. Ding, H., and Demple, B. (2000) Direct nitric oxide signal transduction via nitrosylation of iron-sulfur centers in the SoxR transcription activator. *Proc. Natl. Acad. Sci. U.S.A.* **97,** 5146–5150
21. Hyduke, D. R., Jarboe, L. R., Tran, L. M., Chou, K. J., and Liao, J. C. (2007) Integrated network analysis identifies nitric oxide response networks and dihydroxyacid dehydratase as a crucial target in *Escherichia coli*. *Proc. Natl. Acad. Sci. U.S.A.* **104,** 8484–8489
22. Partridge, J. D., Bodenmiller, D. M., Humphrys, M. S., and Spiro, S. (2009) NsrR targets in the *Escherichia coli* genome: new insights into DNA sequence requirements for binding and a role for NsrR in the regulation of motility. *Mol. Microbiol* **73,** 680–694
23. Crack, J. C., Green, J., Thomson, A. J., and Le Brun, N. E. (2014) Iron-sulfur clusters as biological sensors: the chemistry of reactions with molecular oxygen and nitric oxide. *Acc. Chem. Res.* **47,** 3196–3205
24. Crack, J. C., Munnoch, J., Dodd, E. L., Knowles, F., Al Bassam, M. M., Kamali, S., Holland, A. A., Cramer, S. P., Hamilton, C. J., Johnson, M. K., Thomson, A. J., Hutchings, M. I., and Le Brun, N. E. (2015) NsrR from *Streptomyces coelicolor* is a nitric oxide-sensing [4Fe-4S] cluster protein with a specialized regulatory function. *J. Biol. Chem.* **290,** 12689–12704
25. Ren, B., Zhang, N., Yang, J., and Ding, H. (2008) Nitric oxide-induced bacteriostasis and modification of iron-sulphur proteins in *Escherichia coli*. *Mol. Microbiol.* **70,** 953–964
26. Landry, A. P., Duan, X., Huang, H., and Ding, H. (2011) Iron-sulfur proteins are the major source of protein-bound dinitrosyl iron complexes formed in *Escherichia coli* cells under nitric oxide stress. *Free Radic. Biol. Med.* **50,** 1582–1590
27. Brown, G. C. (2007) Nitric oxide and mitochondria. *Front. Biosci.* **12,** 1024–1033
28. Kennedy, M. C., Antholine, W. E., and Beinert, H. (1997) An EPR investigation of the products of the reaction of cytosolic and mitochondrial aconitases with nitric oxide. *J. Biol. Chem.* **272,** 20340–20347
29. Yang, J., Duan, X., Landry, A. P., and Ding, H. (2010) Oxygen is required for the L-cysteine-mediated decomposition of the protein-bound dinitrosyl iron complexes. *Free Radic. Biol. Med.* **49,** 268–274
30. Tinberg, C. E., Tonzetich, Z. J., Wang, H., Do, L. H., Yoda, Y., Cramer, S. P., and Lippard, S. J. (2010) Characterization of iron dinitrosyl species formed in the reaction of nitric oxide with a biological Rieske center. *J. Am. Chem. Soc.* **132,** 18168–18176
31. Grabarczyk, D. B., Ash, P. A., and Vincent, K. A. (2014) Infrared spectroscopy provides insight into the role of dioxygen in the nitrosylation pathway of a [2Fe2S] cluster iron-sulfur protein. *J. Am. Chem Soc.* **136,** 11236–11239
32. Crack, J. C., Smith, L. J., Stapleton, M. R., Peck, J., Watmough, N. J., Buttner, M. J., Buxton, R. S., Green, J., Oganesyan, V. S., Thomson, A. J., and Le Brun, N. E. (2011) Mechanistic insight into the nitrosylation of the [4Fe-4S] cluster of WhiB-like proteins. *J. Am. Chem. Soc.* **133,** 1112–1121
33. Duan, X., Yang, J., Ren, B., Tan, G., and Ding, H. (2009) Reactivity of nitric oxide with the [4Fe-4S] cluster of dihydroxyacid dehydratase from *Escherichia coli*. *Biochem. J.* **417,** 783–789
34. Tonzetich, Z. J., Do, L. H., and Lippard, S. J. (2009) Dinitrosyl iron complexes relevant to Rieske cluster nitrosylation. *J. Am. Chem. Soc.* **131,** 7964–7965
35. Landry, A. P., Cheng, Z., and Ding, H. (2015) Reduction of mitochondrial protein mitoNEET [2Fe-2S] clusters by human glutathione reductase. *Free Radic Biol. Med.* **81,** 119–127
36. Iwasaki, T., Samoilova, R. I., Kounosu, A., Ohmori, D., and Dikanov, S. A. (2009) Continuous-wave and pulsed EPR characterization of the [2Fe-2S](Cys)3(His)1 cluster in rat MitoNEET. *J. Am. Chem. Soc.* **131,** 13659–13667

37. Bak, D. W., Zuris, J. A., Paddock, M. L., Jennings, P. A., and Elliott, S. J. (2009) Redox characterization of the FeS protein MitoNEET and impact of thiazolidinedione drug binding. *Biochemistry* **48,** 10193–10195
38. Watanabe, S., Kita, A., Kobayashi, K., and Miki, K. (2008) Crystal structure of the [2Fe-2S] oxidative-stress sensor SoxR bound to DNA. *Proc. Natl. Acad. Sci. U.S.A.* **105,** 4121–4126
39. Fitzpatrick, J., and Kim, E. (2015) Synthetic modeling chemistry of iron-sulfur clusters in nitric oxide signaling. *Acc. Chem. Res.* **48,** 2453–2461
40. Tsai, M. L., Tsou, C. C., and Liaw, W. F. (2015) Dinitrosyl iron complexes (DNICs): from biomimetic synthesis and spectroscopic characterization toward unveiling the biological and catalytic roles of DNICs. *Acc. Chem. Res.* **48,** 1184–1193
41. Dicus, M. M., Conlan, A., Nechushtai, R., Jennings, P. A., Paddock, M. L., Britt, R. D., and Stoll, S. (2010) Binding of histidine in the (Cys)(3)(His)(1)-coordinated [2Fe-2S] cluster of human mitoNEET. *J. Am. Chem. Soc.* **132,** 2037–2049
42. Wu, G., Liu, W., Berka, V., Tsai, A.-L. (2015) H-NOX from *Clostridium botulinum*, like H-NOX from *Thermoanaerobacter tengcongensis*, binds oxygen but with a less stable oxyferrous heme intermediate. *Biochemistry* **54,** 7098–7109
43. Huang, L., Abu-Soud, H. M., Hille, R., and Stuehr, D. J. (1999) Nitric oxide-generated P420 nitric oxide synthase: characterization and roles for tetrahydrobiopterin and substrate in protecting against or reversing the P420 conversion. *Biochemistry* **38,** 1912–1920
44. Sarraf, S. A., Raman, M., Guarani-Pereira, V., Sowa, M. E., Huttlin, E. L., Gygi, S. P., and Harper, J. W. (2013) Landscape of the PARKIN-dependent ubiquitylome in response to mitochondrial depolarization. *Nature* **496,** 372–376
45. Kusminski, C. M., Chen, S., Ye, R., Sun, K., Wang, Q. A., Spurgin, S. B., Sanders, P. E., Brozinick, J. T., Geldenhuys, W. J., Li, W. H., Unger, R. H., and Scherer, P. E. (2016) MitoNEET-Parkin effects in pancreatic α- and β-cells, cellular survival, and intrainsular cross talk. *Diabetes* **65,** 1534–1555
46. Shimberg, G. D., Michalek, J. L., Oluyadi, A. A., Rodrigues, A. V., Zucconi, B. E., Neu, H. M., Ghosh, S., Sureschandra, K., Wilson, G. M., Stemmler, T. L., and Michel, S. L. (2016) Cleavage and polyadenylation specificity factor 30: an RNA-binding zinc-finger protein with an unexpected 2Fe-2S cluster. *Proc. Natl. Acad. Sci. U.S.A.* **113,** 4700–4705
47. Cowart, R. E., Singleton, F. L., and Hind, J. S. (1993) A comparison of bathophenanthrolinedisulfonic acid and ferrozine as chelators of iron(II) in reduction reactions. *Anal. Biochem.* **211,** 151–155
48. Siegel, L. M. (1965) A direct microdetermination of sulfide. *Anal. Biochem.* **11,** 126–132